a decade of research

XEROX PALO ALTO RESEARCH CENTER

1970-1980

edited by giuliana lavendel
with the assistance of carol leitner
and the staff of the palo alto
technical information center

R. R. BOWKER COMPANY
New York & London, 1980

Most of the articles in this volume have been or will be published in other publications (as indicated in the Contents). All articles are reprinted with permission.

Published by R. R. Bowker Company
1180 Avenue of the Americas, New York, N.Y. 10036

International Standard Book Number 0-8352-1327-7
Library of Congress Catalog Card Number 80-68031

Printed and bound in the United States of America

contents

High Speed Laser Printing Systems *(excerpted)*

by
Gary K. Starkweather
Xerox Corporation - Palo Alto Research Center

Introduction

The advent of the continuous wave laser has enabled many technologies to advance significantly, especially high speed image recording. The very high radiance of the laser as well as the highly directional and confined beam that it emits has permitted technologies that have been known for years to move from the laboratory curiosity stage to the product environment. Flying spot scanning technology has been one major benefactor of the laser and the technologies that it has enabled. A high speed laser scan system can be used to produce images that are both pleasing to the user and are at least the equal of images generated by printing as well. Such technology is utilized by the Xerox 9700 electronic printer. The full text of this paper will appear as a chapter in Laser Applications by Joseph Goodman (Academic Press, forthcoming). A schematic of the full system is shown as Figure 1.

Polygonal Scanners

The polygonal scanner might appear as the most primitive of the deflection technologies available for high speed scanning. Polarization effects, the interaction of light with sound, etc., are clearly more advanced than a multifaceted mirror on the end of a motor. The fact is, however, that even for medium speed applications and especially for high speed printer applications, this technology outclasses all competitors to date.

The available scan angle from a polygonal mirror of K facets can be shown to be

$$\Theta = 720/K \text{ degrees} \qquad (1)$$

This is so since the mirrors are on the circumference of a circle and if there are K mirrors, then each mirror must subtend 360/K degrees from the center of rotation. For obvious reasons, this equation does not apply when K has a value of 1 or 2. Furthermore, the scan angle is doubled by

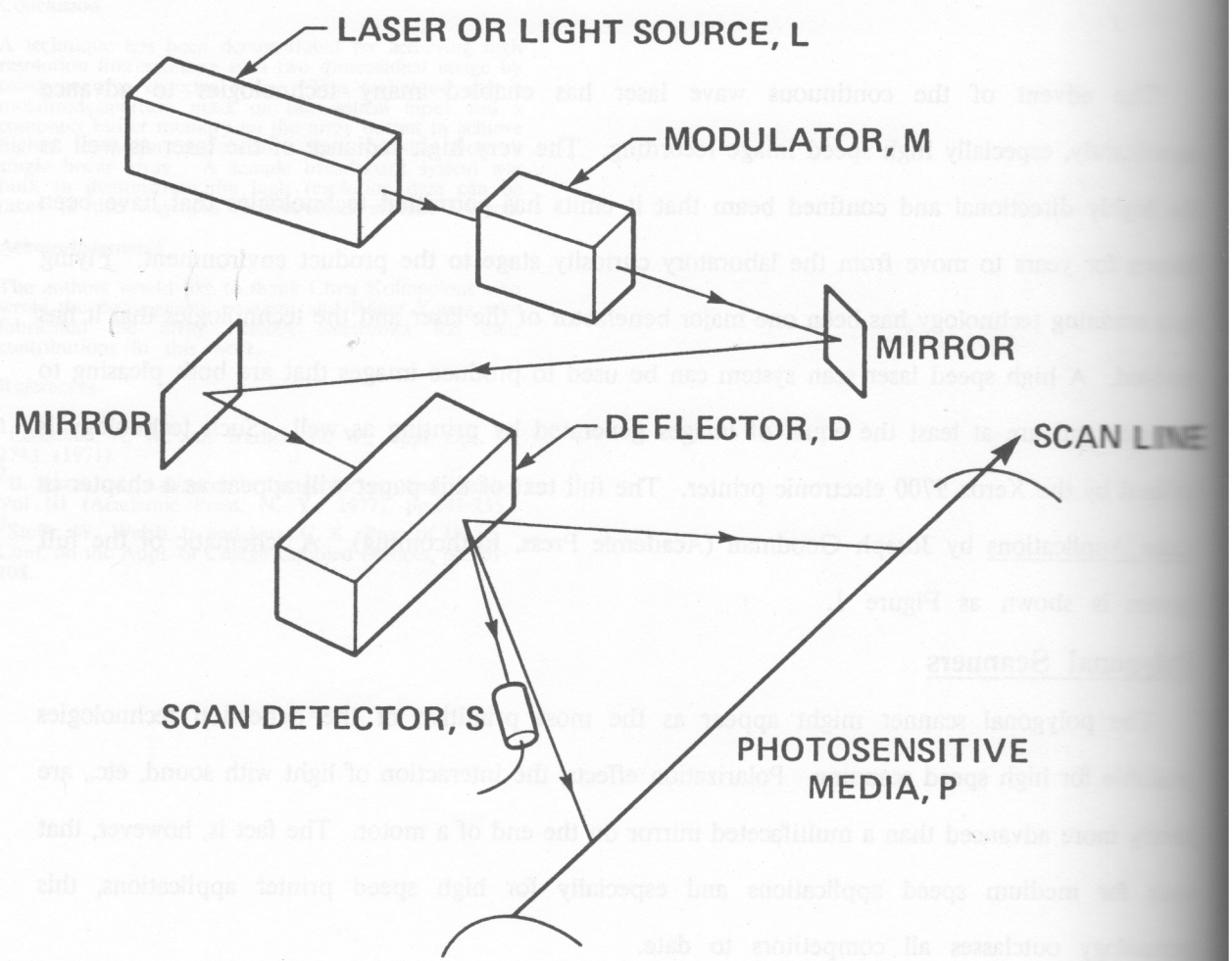
LASER OR LIGHT SOURCE, L
MODULATOR, M
MIRROR
MIRROR
DEFLECTOR, D
SCAN LINE
SCAN DETECTOR, S
PHOTOSENSITIVE
MEDIA, P

FIGURE 1

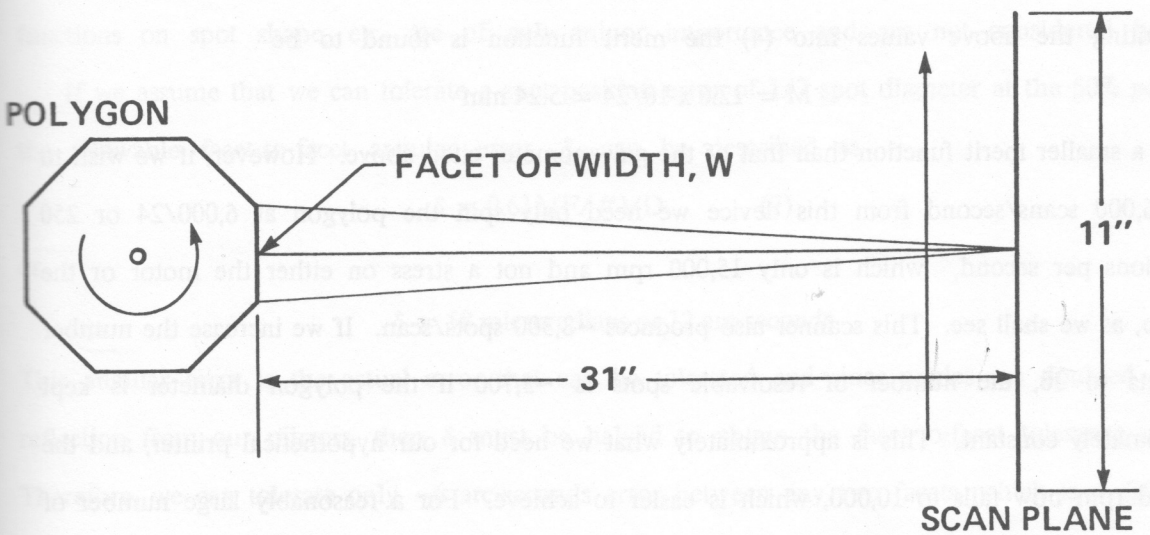

FIGURE 2

reflection as in galvanometers, giving 720/K as the scan angle per facet. The minimum resolvable angle, α

$$\alpha = 1.22\,\lambda/W \qquad (2)$$

can be used to derive N_r for a polygonal scanner of K facets and facet width W. For a Gaussian beam, the relation

$$N_r = 12.6\,W/\lambda K \qquad (3)$$

can be derived. For W = 1 cm, K = 24 and λ = 0.633 nm, equation (3) yields

$$N_r = 8294 \text{ spots}$$

The merit function, M, can be shown to be

$$M = 12.6\,W/K \qquad (4)$$

Substituting the above values into (4) the merit function is found to be

$$M = 12.6 \times 10/24 = 5.24 \text{ mm}$$

This is a smaller merit function than that of the galvanometer cited above. However, if we wish to make 6,000 scans/second from this device we need only spin the polygon at 6,000/24 or 250 revolutions per second, which is only 15,000 rpm and not a stress on either the motor or the polygon, as we shall see. This scanner also produces ~8,300 spots/scan. If we increase the number of facets to 36, the number of resolvable spots is ~3,700 if the polygon diameter is kept approximately constant. This is approximately what we need for our hypothetical printer, and the required rpm now falls to 10,000, which is easier to achieve. For a reasonably large number of facets, K, the polygon diameter D is

$$D = W\,K/\pi \qquad (5)$$

Thus our 36 facet polygon having 6.67 mm facets is only 76 mm or 3 inches in diameter.

The polygonal scanner has some significant advantages over the galvanometer in that, (a) it has multiple facets to reduce its rotational speed requirements and (b) it moves only in one direction. The unidirectional characteristic of polygonal scanners should in general give them long life.

Until recently, there has been a severe problem with polygonal scanners that limited their volume producibility and cost effectiveness: this is the requirement of facet-to-facet angular uniformities. Assuming we wish to scan an 11" page with our 36 facet scanner, the system geometry requires a polygon-to-scan plane distance of ~31 inches, as shown in Figure 2. With the facet width W of 6.67 mm, and a 31 inch or 787 mm polygon-to-scan plane distance D, the system

or focal ratio is

$$F/\# = 787/6.67 = 118$$

w we consider the facet designed to truncate the imaging beam so that it is uniformly inated, we can approximate the the scan spot size d as

$$d = 1.22\lambda(F/\#) \qquad (6)$$

equation is not strictly correct, since, due to the rectangular facet geometry, the spot size is determined by a $Sinc^2$ function rather than the square of a first order Bessel function. The size differences are minimal, however, and for the purposes of this discussion precise mination is not necessary. For $\lambda = 633$ nm, we have d = 91 micrometers or 3.6×10^{-3} inches e 50% intensity points of the spot; the differences between the Gaussian, Bessel and Sinc ions on spot shape, etc. are of only minor importance and are not considered here. f we assume that we can tolerate a spot position error of 1/2 spot diameter at the 50% points, allowable facet-to-facet angular error, δ, can be described as

$$\delta = 0.61\lambda(F/\#)/D \qquad (7)$$

$$\delta = 58 \text{ microradians or } 12 \text{ arc-seconds}$$

angular error is the actual error that can be tolerated and since angles are doubled upon tion from our mirrors, then δ must be halved to obtain the facet-to-facet tolerance value. efore, we can tolerate only ~6 arc-seconds error between any two facets, which is a difficult nce to achieve in production situations.

chemes have been devised to sense the position of the scan beam at the image plane and use ousto-optical deflector to "steer" the beam to the correct focal position. This complicates the al system and reduces its overall efficiency since another component has been introduced into ight path that has losses from both transmission and reflection. Various techniques, among optical correction schemes by the author and also by Fleischer significantly reduce this lem. As shown in Figure 3, a cylinder lens can be inserted into the optical path of the ning beam to reduce the facet-to-facet angular tolerances by 50 to 100 times. This means that ngular tolerances can now be on the order of arc-minutes, instead of arc-seconds, and the lem is sufficiently corrected to permit low cost polygonal scanners to be used. It should be ully noted that only polygon facet angular errors that produce ray deviations from the scan-

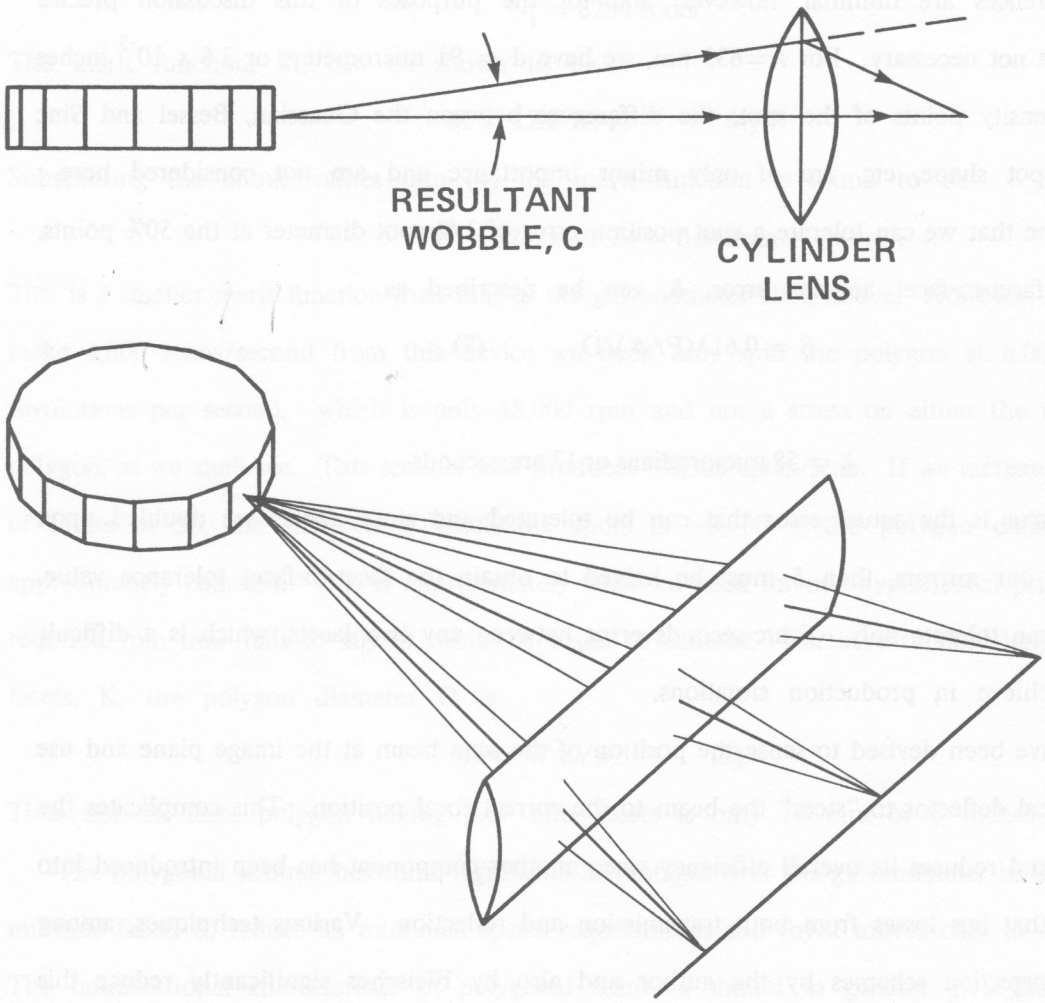

FIGURE 3

plane are corrected by the above technique.

The cylinder functions as follows: the polygon facet acts as the object for the cylinder lens, and the lens therefore images the facet at an image plane that is intended to coincide with the photoreceptor surface. The image dimension in the vertical direction, d_t (called the tangential direction), is therefore the dimension of the illuminated portion of the polygon facet multiplied by the magnification or minification of the optical system. If we define the illuminated height of the facet as A, the cylinder lens to facet distance O and the cylinder lens to photoreceptor or object distance I then the tangential spot dimension is in the first order given by the relation

$$d_t = AI/O \qquad (8)$$

Thus, if we wish to have a final tangential spot size of ~ 0.1 mm at the 50% points and the facet illuminated heigth is 1.0 mm, the system magnification should be 0.1X. Notice that if the facet is improperly positioned and causes the ray to deviate from a plane by some angle δ, the cylinder lens intercepts the ray and redirects it to the image scan line. This obviously corrects the effect of the facet error. Furthermore, this correction scheme is quite foolproof and not subject to malfunction.

With this simple correction scheme, the superior virtues of the polygonal scanner can now be exploited to the fullest with significant cost effectiveness. While the majority of angular errors are to be found in the fabrication of the polygon, this system also corrects for bearing errors etc. Bearing quality can also be relaxed since arc-second polygons require arc-second (class 9) bearings to make use of the fabrication precision.

The polygonal scanner, as mentioned earlier, is basically a disk of material with optical flats on its periphery. When this optical element is rotated at high speed, there are high stresses on the polygon material; the facets "paddle" the air and offer resistance to the rotating power source, the motor. These features need careful assessment in any high speed printing system. Let us consider the polygon requirements for a device printing an 11" wide field and having a resolution of ~400 lines/inch and 400 scans/inch; let us also choose a photoreceptor velocity of 35 inches/second, which results in a printer capable of producing ~4 pages/second. The foregoing specifications are well in excess of any device on the market today and can serve as an excellent test case for polygon scanner technology, keeping in mind that this hypothetical printer would consume data at a minimum rate of 62×10^6 bits/second.

For this discussion, assume a polygon diameter of 3.0 inches or 76.2 mm. This permits the

polygon to have 24 facets of ~1.0 centimeter each. Since our photoreceptor velocity is 35 inches/second and the scan density is 400 lines/inch, the polygon must produce 14,000 scans/second. With 24 facets the polygon rotational rate is ~583 revolutions/second or 35,000 rpm. Schlichting provides the following data for drag on rotating disks. The Reynolds number R is given by the relation

$$R = r^2 \omega^2 \rho / \mu \qquad (9)$$

where r is the disk or polygon radius, ω is the disk angular velocity, ρ is the air density and μ the air viscosity. We shall also define a coefficient C_m which is related to the Reynolds number R by the relation

$$C_m = 3.87/R^{1/2} \qquad (10)$$

which holds for a laminar flow region, and should be sufficient for our needs. The torque required to compensate for windage can be shown to be

$$T = C_m \rho \omega^2 r^5/2 \text{ ounce-inches} \qquad (11)$$

Lastly, the power required to overcome the windage losses can be

$$P = TZ/1351.75 \text{ watts} \qquad (12)$$

where Z is the rpm and the torque T is in ounce-inches. The units in (11) and (12) are purposely mixed since most motor specifications carry ounce-inch torque specifications rather than newton-meters. The coefficient C_m is dependent on many variables: for example, if the polygon is in a tight enclosure, the constant changes from 3.87 to ~2.67 etc, but if turbulent flow is encountered, the coefficient expression changes. For our purposes, however, let us assume equation (10) to be valid for this discussion.

The generally accepted value or the Reynolds number R at which transition from laminar to turbulent flow occurs is 3×10^5. Also, the density of air ρ decreases with temperature while the kinematic viscosity μ increases. Substituting the appropriate values and constants, the Reynolds number becomes 3.2×10^5, which is slightly above the laminar region. The torque T turns out to be 1.0 ounce-inches for a "free" or unenclosed polygon. Therefore the power, as per equation (12), amounts to

$$P = (1.0)(35{,}000)/1351 = 26 \text{ watts}$$

It is interesting to note that a printer running at half speed (17.5 inches/second) with the other parameters the same as above, requires an rpm of only 17,500, the Reynolds number is only

1.4×10^5, and the resulting torque drops dramatically to 0.21 ounce-inches, while the power amounts to only 2.7 watts. Thus windage losses can be relatively high, depending on rotor diameter and rpm: should the rotor diameter be 4 inches instead of 3 inches, for example, the power required at 35,000 rpm is 100 watts. This power loss may produce unpleasant acoustical effects, which must be disturbed to prevent environmental disturbances. The more facets present on the disk periphery, the quieter the rotor, since the apex joining the two facets does not project as far into the laminar or turbulent flow in the vicinity of the polygon surface. To some extent, the faceted nature of the polygon invalidates the disk approximation used in equation (11) above, but the error introduced by the flat facets is not substantial.

Beyond air frictional effects, motor bearings must also be considered as a source of friction. Whether one uses air bearings, grease bearings or the more conventional ball bearings is a matter of choice. Air bearings offer the quietest operation and the least frictional resistance, while greased journal bearings would probably be stiff, and the highest power consumers. The range of power requirements for the various bearing types varies from a low of about 4 watts for air bearings to a high of ~25 watts for a greased journal bearing at our design rpm of 35,000.

The choice of bearing type, and its precision requirements, will depend on how much the optical or electro-optical subsystem can tolerate facet "wobble." Rotor unbalance is crucial as well with regards to vibration and bearing life.

We must now look at the rotational stresses that our polygon undergoes while spinning in excess of 580 revolutions per second. The disk periphery is moving at 458 feet/second or ~Mach 0.5. Since our polygon must be mounted to the driving motor via its shaft, a center bore in the polygon material must be provided. The polygon therefore becomes a spinning annulus, whose stress can be shown as

$$S_t = (7.1 \times 10^{-6}) w Z^2 [(3+m)R_o^2 + (1-m)R_i^2] \qquad (13)$$

where w is the weight of the rotor material in pounds per cubic inch, Z is the rpm, R_o is the outer radius, R_i the inner radius and m is Poisson's ratio. Equation (13) can be solved for the rpm Z at which the stress S_t equals the yield stress of the material being used, with S_t usually given in pounds. This would result in a maximum value of Z for the rotor parameters used. Assuming that $R_o^2 > R_i^2$ and making m = 0.3 (a good approximation) we can rewrite (13) as

$$Z_{max} = (4.27x10^4 S_t/wR_o^2)^{1/2} \qquad (14)$$

If we use the parameters for our ~3 inch rotor, we can generate a table comparing the performance of various materials; such a comparison is shown in Table I.

Copper and brass, even though easy materials to work with mechanically, provide poor spinner materials; glass and stainless steel (#51430) are roughly identical. Our polygon could be made out of crown glass with a safety factor of about 2, with type 7075 Aluminum which has the greatest margin of safety among the materials considered; our 24 facet polygon could produce about $1.7x10^8$ spots/second at maximum Z. Beryllium could be the best from a performance standpoint, being able to generate over $3x10^8$ spots/second, but it has a high toxicity when machined, and is also expensive; unless rpm's in excess of 70,000 (2x safety factor) are required, beryllium is not to be considered. Surface profiles of the polygon mounting hole make a great deal of difference in the ultimate rpm capabilities of the device: rather than the maximum attainable performance, cost/performance is crucial for product planning. The material chosen should have (a) high strength-to-density ratio, (b) low density, (c) low Poisson's ratio, (d) low thermal expansion coefficient, and (e) be somewhat ductile and (f) very stable.

We should also concern ourselves with the rotation mechanism. While one could drive the polygon from an air turbine, this might be unduly noisy. An electric motor is clearly best for the rpm regimes we are considering; how the motor is driven, how the rpm is stabilized, windage losses, bearing losses, and acceleration requirements will determine the ultimate power requirements of the polygon motor; they need not be very large for most practical systems.

In sum, the polygon handles the laser beam deflecting task very well: no particular aspect of rotor or driver technology need be extended to provide the required spot size and data rate demanded by the 9700. While the future may well provide electro-optical or other successors to the polygon deflector, all current high speed printing technologies use the multi-faceted polygon as the prime beam deflection mechanism.

Printer Optical Systems

We shall now discuss some of the characteristics of the 9700 optical system. While lens design is not speed dependent, the modulator and deflector are affected by the data rate and the printer optical system must produce small optical spots at a high data rate. The highest data rate prevalent

Selected Polygon Materials

Material	Yield Strength (psi)	Density (lbs/cu.in.)	Poissons Ratio	Maximum R.P.M.
Aluminum 7075-T6	73,000	0.101	0.334	123,000
Stainless Steel 51430	60,000	0.28	0.300	67,000
Copper	17,000	0.321	0.340	33,000
Brass	16,000	0.302	0.340	33,000
Glass	20,000	0.09	0.210	69,000
Beryllium	40,000	0.066	0.250	110,000

Outer Radius = 1.43 inches
Inner Radius = 0.25 inches

Table I

in printing today is ~20 Mbits/second (Xerox 9700). We have seen the modulator and polygon characteristics that are required for this performance level and we shall also look at the optical system light throughput to achieve the required exposure at the photoreceptor.

As shown in Figure 4, the light from the laser activates some "beam conditioning" optics that focus the light for appropriate modulator rise time performance. The laser in this case is a He-Cd type of proprietary design, combined with a non-red sensitive photoreceptor; the xerographic marking engine is derived from the Xerox 9200 copier/duplicator. The He-Cd laser has a power output of about 10-15mW; it permits a larger permissible imaging f/# for the same desired image spot size than the Ne laser. Moreover, the 9700 uses the He-Cd laser to utilize the 9200 marking engine technology.

The light from the modulator passes to a cylinder lens whose power plane is oriented orthogonally to the direction of scan and then to a spherical lens. The light then is reflected by the polygon, on to the correction cylinder lens, and from there to the photoreceptor. The first cylinder lens (pre-polygon), spherical lens and correction lens form an anamorphic imaging system, which is intended to produce a rounded spot at the photoreceptor. Thus component separation can be realized, and some significant polygon advantages obtained. One principal advantage is that more than one facet is illuminated, in fact nearly three are simultaneously illuminated, as shown in Figure 5.

As depicted in the figure, the scanning facet moves through a field or line of light, and thus the entire facet width does the imaging. Duty cycle is very high since the facet is illuminated during its entire scan traversal; typical scan duty cycles are 90% and higher in practice.

This technique is obviously wasteful of light, but xerographic sensitivity is tolerant of this one architectural drawback. The principal advantage is that the polygon turns out to be quite small. For example, if the spot size is chosen to be ~0.03 inches or 76 micrometers at the 50% points then the required f/# for the He-Cd wavelength of 442 nm is ~140 as determined from equation (6). Thus if the the polygon-to-scan plane distance is ~35 inches, the required facet width would be

$$W = 35/140 = 0.25 \text{ inches}$$

An 11 inch scan line subtends an angle of 18°, when produced by a polygon at a distance of 35 inches from the scan plane. If we use a 36-facet polygon, then by equation (1), the maximum scan angle is found to be 20 inches. Thus a 36-facet polygon would have a scan efficiency of 90% (18

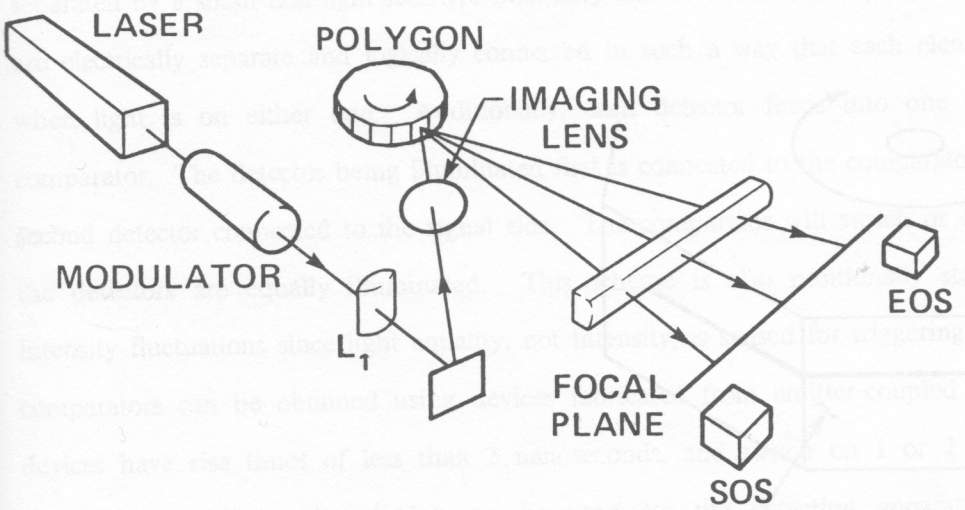
LASER
POLYGON
IMAGING
LENS
MODULATOR
L_1
EOS
FOCAL
PLANE
SOS

FIGURE 4

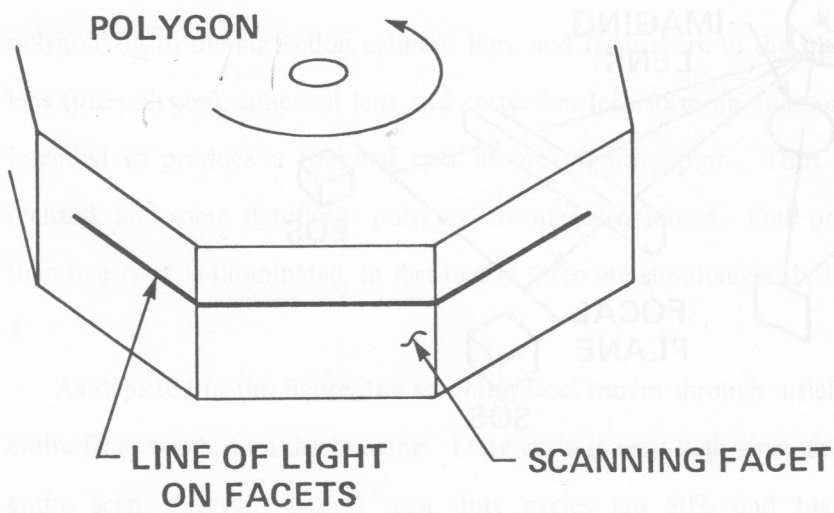

FIGURE 5

inches/20 inches) and be only 2.86 inches in diameter. The multiplicity of facets also means that, at the 9700 process speed of 20 inches/second, an rpm of only 10,000 is required, which is very straightforward with this size of polygon.

Also shown in Figure 4 is the start-of-scan detector, which senses the scan beam prior to its passage onto the appropriate area of the photosensitive surface. Since the digital data buffer must be "triggered" or "clocked" synchronously with the optical writing beam, some form of beam position detection is necessary. The 9700 system uses a separate detector for this purpose: it should be a "fast" system because successive bits occur every ~50 nanoseconds. For a synchronization start precision of 1/4 bit, the detector must have an optically and electronically precise risetime of ~12 nanoseconds. As shown in Figure 6, a detector having two sensitive areas separated by a small non-light-sensitive boundary can be used for this purpose. The detector areas are electrically separate and logically connected in such a way that each element is enabled only when light is on either one. Additionally, each detector feeds into one of two inputs of a comparator. The detector being illuminated first is connected to the comparator reference, with the second detector connected to the signal side. The comparator will switch or deliver a pulse when the detectors are equally illuminated. This scheme is also positionally stable with respect to intensity fluctuations since light equality, not intensity, is sensed for triggering purposes. Very fast comparators can be obtained using devices fabricated from emitter-coupled logic (ECL): these devices have rise times of less than 2 nanoseconds, and switch on 1 or 2 millivolt differences.

Typically, silicon photodiodes can be used for the detection apparatus. At the He-Ne wavelength of 633 nm, silicon photodiodes have a sensitivity of ~0.6 amperes/watt. Thus if the laser writing beam has a power of ~1 mW, then the the signal across a 50Ω load resistor would be ~30 millivolts, which is more than adequate to drive an appropriately designed amplifier and the comparator. This scheme is not the only way in which to scan-detect and trigger but is presented as a workable scheme that is used on the Xerox 9700 printer.

We can also do some comparisons by modeling a simple optical scanning system and observing its overall efficiency, as shown in Figure 7. This system is composed of the laser, two pre-modulator lenses for beam "conditioning", the modulator, three more imaging lenses and the polygon, plus a minimum of three mirrors of reflectance R. If the transmission of each lens in the system is T, the mirror reflectance losses R, the modulator net diffraction efficiency E, and the

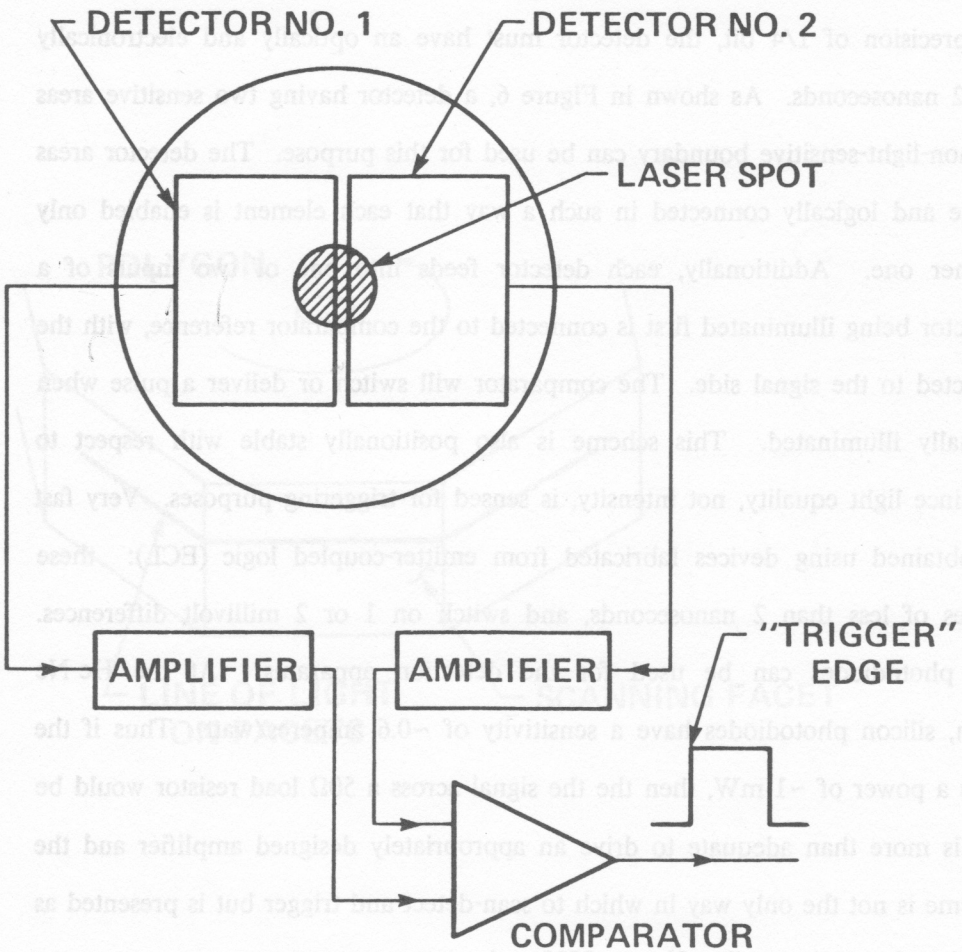
DETECTOR NO. 1
DETECTOR NO. 2
LASER SPOT
AMPLIFIER
AMPLIFIER
"TRIGGER" EDGE
COMPARATOR

FIGURE 6

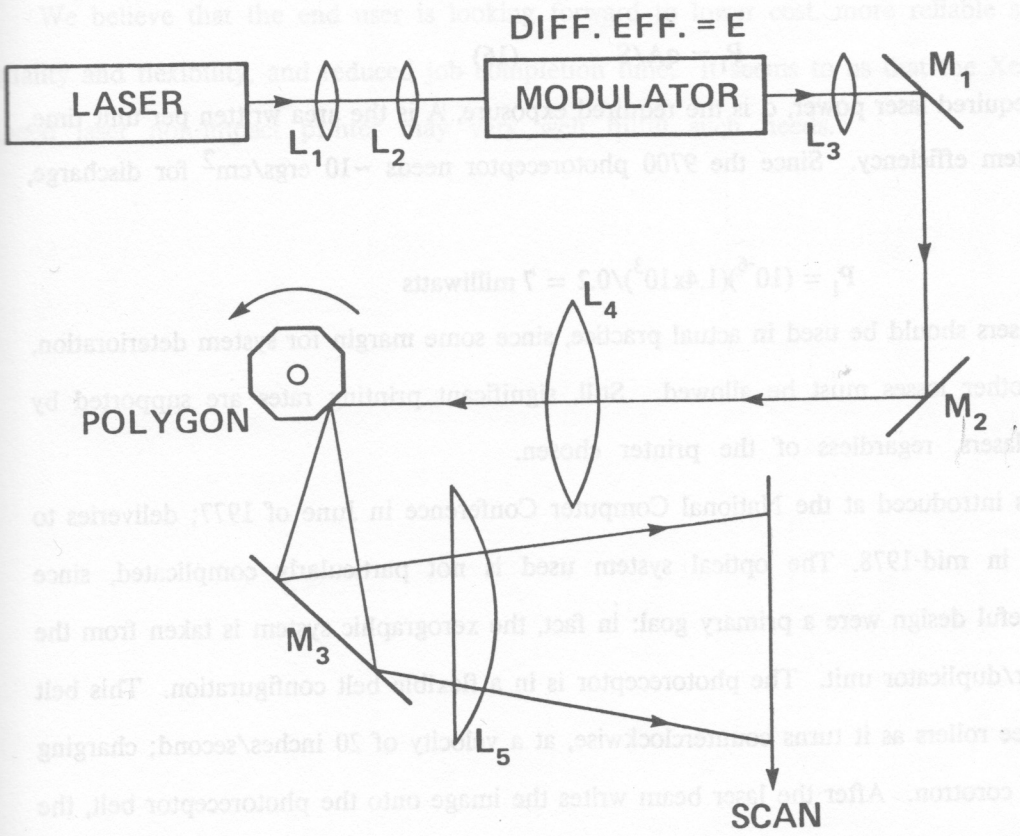

FIGURE 7

polygon efficiency, including configurational losses is P, the net system efficiency S is

$$S = T^5R^3EP \qquad (15)$$

Letting the average lens transmittance T and mirror reflectance R equal 0.93, while the modulator efficiency equals 0.8, the value of S is given by

$$S = (0.93)^8(0.8)P = 0.45P$$

It is interesting to note that if the value is slightly reduced to 0.9, then S becomes 0.34P, or 24% less light throughput. If the polygon efficiency is 0.4, as in the Xerox 9700, then S equals ~20%.

If we now compare the actual laser power required for exposure we can use the following relation

$$P_1 = qA/S \qquad (16)$$

where P_1 is the required laser power, q is the required exposure, A is the area written per unit time, and S is the system efficiency. Since the 9700 photoreceptor needs ~10 ergs/cm^2 for discharge, then

$$P_1 = (10^{-6})(1.4x10^3)/0.2 = 7 \text{ milliwatts}$$

More powerful lasers should be used in actual practice, since some margin for system deterioration, laser aging and other losses must be allowed. Still, significant printing rates are supported by relatively small lasers, regardless of the printer chosen.

The 9700 was introduced at the National Computer Conference in June of 1977; deliveries to customers began in mid-1978. The optical system used is not particularly complicated, since simplicity and careful design were a primary goal: in fact, the xerographic system is taken from the Xerox 9200 copier/duplicator unit. The photoreceptor is in a flexible belt configuration. This belt passes around three rollers as it turns counterclockwise, at a velocity of 20 inches/second; charging is performed by a corotron. After the laser beam writes the image onto the photoreceptor belt, the exposed image is developed and transferred to the topmost portion of the belt. From one of two paper supplies at the rear of the machine, individual sheets of paper move along the top.

Charged area xerographic development is the marking technique used in the 9700; instead of characters being written by the laser beam, all the area around the characters is discharged. The printer runs at a resolution of 300 bits/inch or 90,000 bits/square inch. Combined with the sophisticated character generator, this increased resolution allows the forms to be produced digitally instead of optically, as in competitive equipment. The text and forms are thus combined as a video

stream for subsequent laser modulation, and this permits pre-collation of the document. Form quality can be quite high, and approximately 800 pages can be stored on the system's magnetic disk. Maximum printer line rate is 18,000 lines/minute.

The 9700 represents an interesting technology: it is capable of emulating a line printer, but it clearly has far more capabilities, and its potential for high quality electronic image generation is obvious. Since there is no need to store preprinted forms, costly overhead is eliminated in many cases; however, specific applications will obviously determine the utility and cost effectiveness of such features.

We believe that the end user is looking forward to lower cost, more reliable systems, better quality and flexibility, and reduced job completion time. It seems to us that the Xerox 9700 high speed laser non-impact printer may very well fulfill such needs.

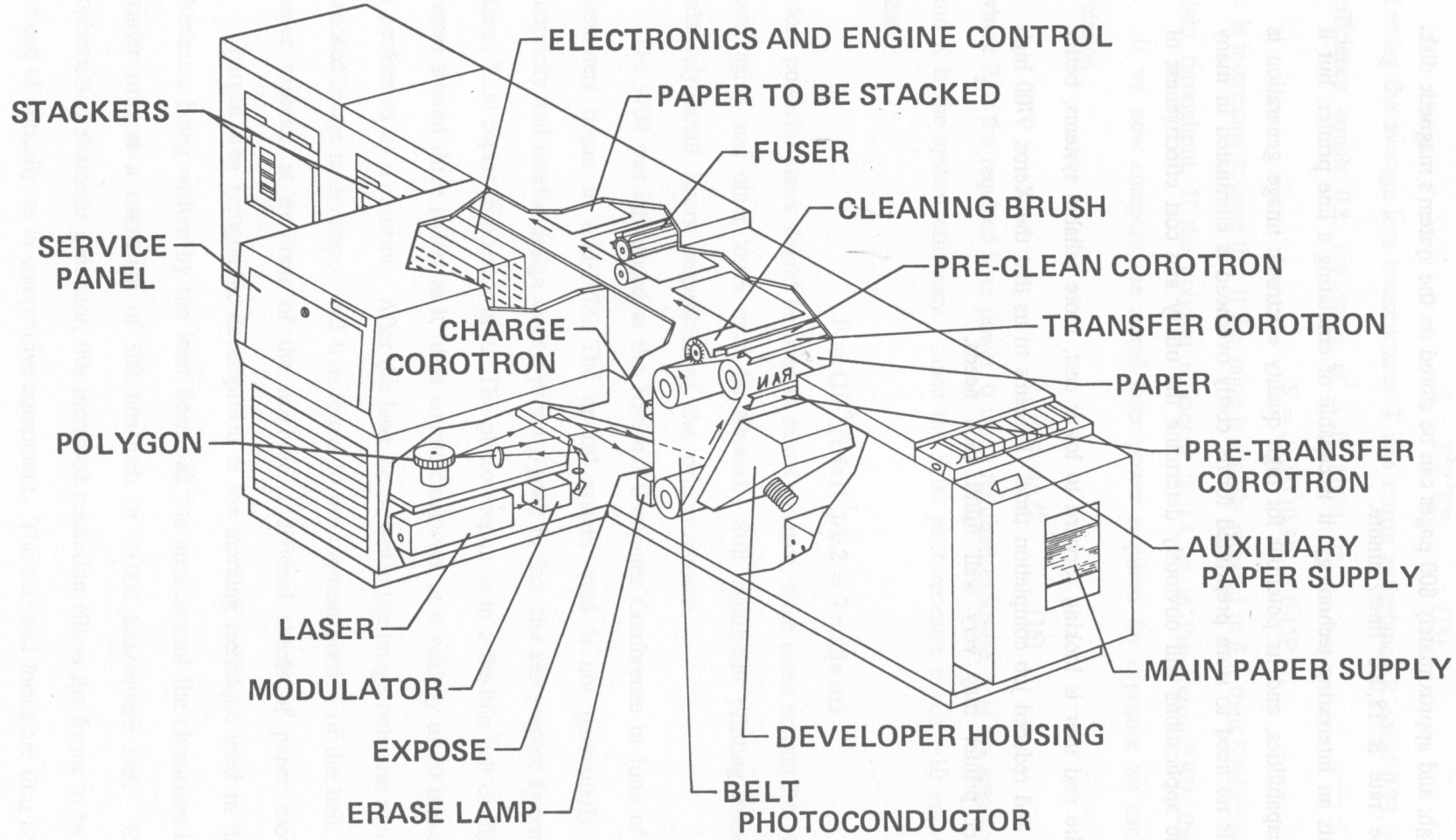
ELECTRONICS AND ENGINE CONTROL
PAPER TO BE STACKED
STACKERS
FUSER
CLEANING BRUSH
SERVICE PANEL
PRE-CLEAN COROTRON
TRANSFER COROTRON
CHARGE COROTRON
PAPER
POLYGON
PRE-TRANSFER COROTRON
AUXILIARY PAPER SUPPLY
LASER
MODULATOR
MAIN PAPER SUPPLY
DEVELOPER HOUSING
EXPOSE
ERASE LAMP
BELT PHOTOCONDUCTOR

FIGURE 8

LIST OF FIGURES

REFERENCES

Born, M. and E. Wolf. Principles of Optics, New York: Pergamon Press, 1975.

Buzzard, R.J. "Gas Lasers for Information Handling - A Review," *Optical Engineering*, Vol. 15 (March/April 1976).

Chen, I. "Electrophotographic Characteristics of Overcoated Photoreceptors," *Photographic Science and Engineering*, Vol. 22 (March/April 1978).

Claus, C.J. "Electrophotographic Processes and Materials," *Image Technology*, (April/May 1969).

Crews, R.W. and P. Rice. "The Videograph Tube - A New Component for High Speed Printing," *I.R.E. Transactions on Electron Devices*, Vol. ED-8 (September 1961).

Cunniff, J.C. "Scanning with Integrated Optics," *Optical Engineering*, Vol. 12 (March/April 1973).

Fleischer, J. US Patent # 3,750,189.

Hance, H.V. and J.K. Parks. Measurement of Light-Sound Interaction Efficiencies in Solids," *Acoustical Society of America, Journal*, Vol. 38 (July 1965).

Korpel, A., R. Adler, P. Desmares and W. Watson. "A Television Display Using Acoustic Deflection and Modulation of Light," *Proceedings of the IEEE*, Vol. 54 (October 1966).

Lucero, J.A., J.A. Duardo and R.V. Johnson. "The Effect of Laser Beam Transverse Mode and Polarization Properties on A-O Modulator Performance," *Society of Photo-Optical Instrumentation Engineers, Transactions*, Vol. 90 (1976).

Meimel, R.F. Mechanics of the Gyroscope, New York: Dover Publications, 1950.

Roetling, P.G. "Binary Approximation of Continuous Tone Images," *Photographic Science and Engineering*, Vol. 21 (March/April 1977).

Schlichting, H. Boundary Layer Theory, New York: McGraw-Hill Co., 1968.

Starkweather, G.K. US Patent #4,040,096.